IEEE MONTECH'86 Conférence sur les antennes et les communications • 29 septembre - 1er octobre 1986
Conference on Antennas and Communications • September 29 - October 1, 1986

SHIELDING EFFECTS OF A GIGANTIC ANTENNA BY TERRAIN

Tadashi Takano, Hiroshi Saitoh and Tomonao Hayashi
The Institute of Space and Astronautical Science
4-6-1 Komaba, Meguro-ku, Tokyo, 153 Japan

Peculiarities due to an antenna shielding by terrain were observed in the operration of the 64 meter diameter antenna. The phenomena were investigated experimentally using Japan's probes to Halley's comet and analyzed theoretically.

Introduction

A gigantic antenna with a 64 m diameter dish was constructed in the Usuda Deep Space Center, Japan in 1984. Its first role was to track two Japan's spacecraft SAKIGAKE and SUISEI which encountered succesfully Halley's comet in March, 1986[1].

The antenna site was chosen in a mountainous area to isolate from artificial radio noises. As the antenna is surrounded by mountains, communication's period is restricted by the time when spacecraft goes across the skyline. In the operation,such phenomena as gradual increase or decrease of reception level, and specific pointing error of the antenna are observed around the crossing time. These phenomena may occur for gigantic antennas for radio astronomy, deep space communications and satellite communications.

This paper describes observed results, and theoretical analysis to clarify that the phenomena are caused by antnenna shielding effects by terrain.

Antenna and its topographic circumstances

The gigantic antenna at Usuda is shown in Fig. 1. It is a cassegrain type antenna installed on an elevation(El)-over-azimuth(Az) mount. The height of elevation axis is 33 m. The antenna gain is 62.6 dB at 2293 MHz which corresponds to 77% efficiency. Half power beamwidth is 0.13 deg., and pointing accuracy of 0.003 deg.RMS is verified. The radio wave from the spacecraft is circularly polarized.

The antenna can be pointed to the target in each following mode:
1) PRD mode: The antenna is controlled by a super-computer which generates the orbit data of the target.
2) AUTO mode: Antenna tracking signal is generated by autotrack system[2].
3) SLAVE mode: The antenna slaves to another tracking antenna.
4) MANU mode: The antenna can be controlled by manual setting of parameters.

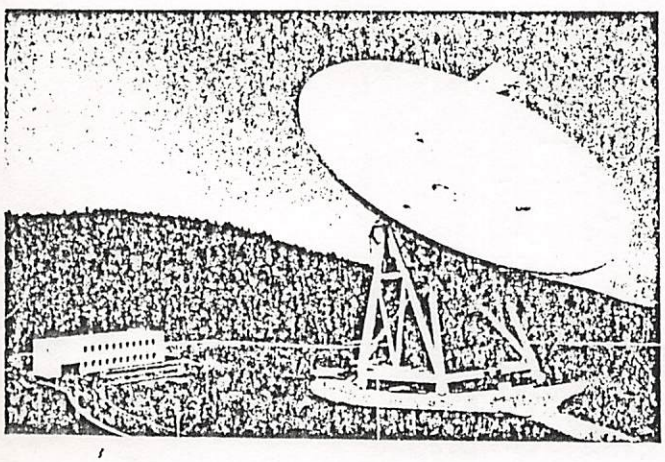

Fig.1 A view of the Usuda Deep Space Center and 64 meter diameter antenna

The autotrack system is designed to operate above the power level of -150 dBm at the input port of the succeeding low noise amplifier. The performance has been verified at sufficiently high elevation angle.

The station is situated about 100 km north from Mt.Fuji, and is at the head of a small river whidch pours into a large basin. The skyline seen from the elevation axis of the main dish is shown in Fig.2. Three sides of north, south and west face to mountains. The west is the direction of the valley head, and the northeast corresponds to the outlet of the river.

The spacecraft appeared at the time of acquisition of signal(AOS) from southeast which corresponds to the mountain 550 m apart and 150 m higher than the site level. The direction of the spacecraft at the time of loss of signal(LOS) was southeast and there are mountain ranges which are 1500 to 4000 m apart and 380 to 800 m higher than the site. Spacecraft directions in both cases change depending on the relative location of the spacecrft and the earth in space.

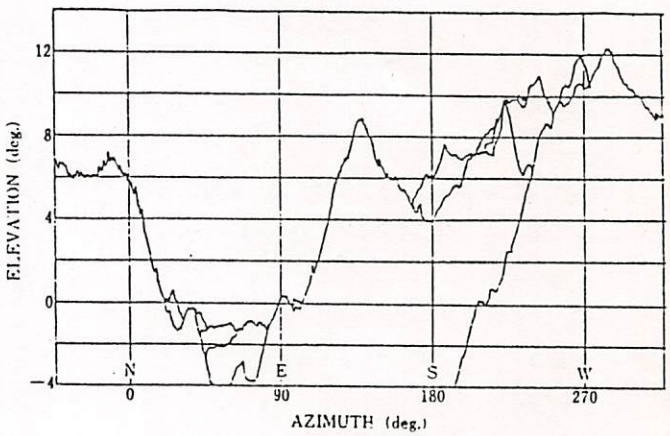

Fig.2 The skyline surrounding the gigantic antenna

Operational results

Typical changes of received carrier level at the time of AOS is shown in Fig.3 for SUISEI. The orbit is shown in Fig.4 in relation to the skyline. At the predicted time when the spacecraft goes across the skyline, the level is 5 dB lower than the value at sufficiently high elevation angle . Then the level increases gradually. It takes 20 minutes after the crossing time to reach the invariable level.

At the time of LOS, the carrier level variation and the spacecraft orbit are shown in Fig.5 and Fig.6 respectively. The level begins to fall down before the predicted crossing time and it remains finite for 2.5 minutes after the time.

The time constant of the change at AOS and LOS are different each other. The level for a period from AOS to LOS changes according to spacecraft-earth slant range, and agrees well with the calculated value from the spacecraft EIRP, receiving facilities capabilities and propagation parameters.

At the low elevation angle, the antenna in AUTO mode showed discrepancy between the real angles and the predicted angles sent from the super-computer for both of elevation and azimuth. It was more significant at LOS than at AOS because of the

TH0156 - 0/86/0000 - 0205 $01.00 C 1986 IEEE

characteristics of the phase-locked receiver. As an example, the data of error angles (predicted value-measured value) are shown in Fig.7. The changes of the angle difference reach 0.10 deg. upward and 0.08 deg. left for El and Az resapecctively, though the angle difference for El seems to include constant offset value.

In order to investigate the relation between the real angles and the reception level, the antenna was switched between PRD mode and AUTO mode. The received carrier levlel in PRD mode is higher then in AUTO mode. It is concluded, therefore, that the real angle in AUTO mode does not point the angle of the maximal power recption.

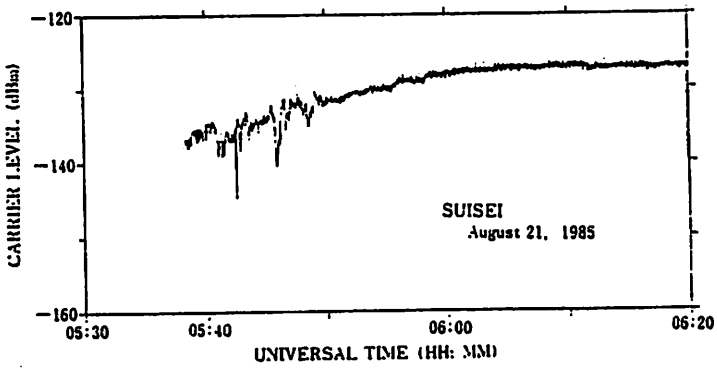

Fig.3 Received power level change at AOS

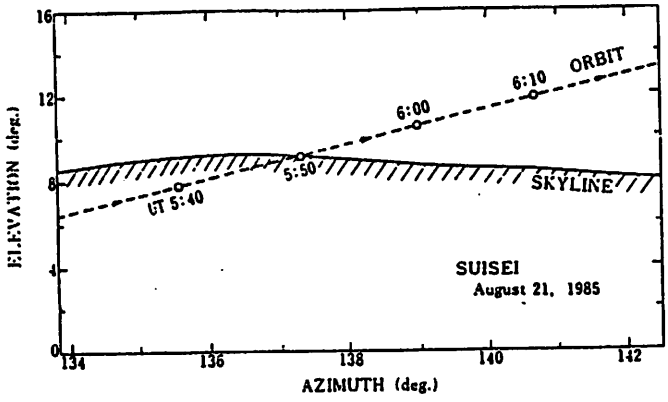

Fig.4 The orbit of the spacecraft and the nearby skyline at AOS

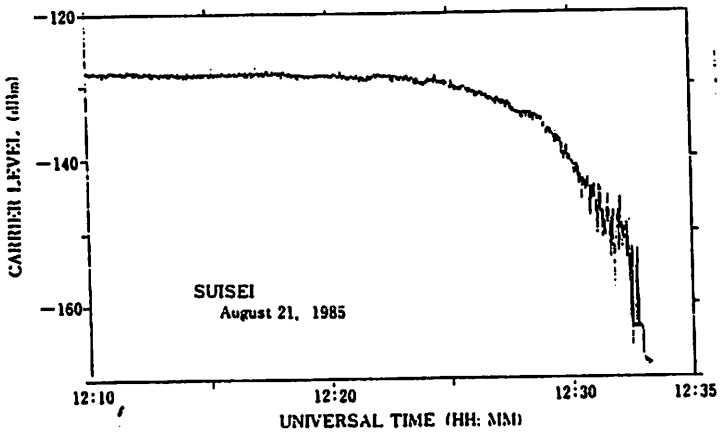

Fig.5 Received power level change at LOS

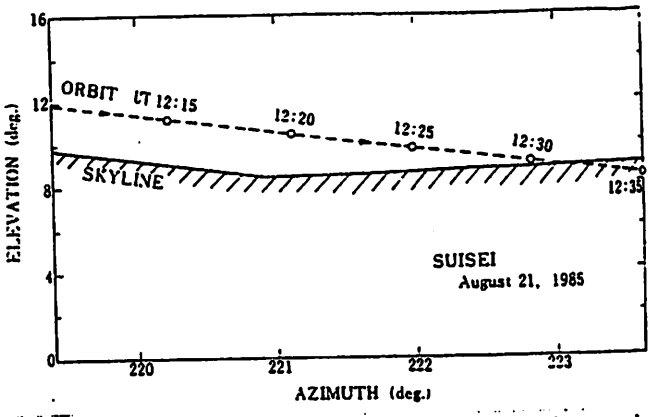

Fig.6 The orbit of the spacecraft and the nearby skyline at LOS

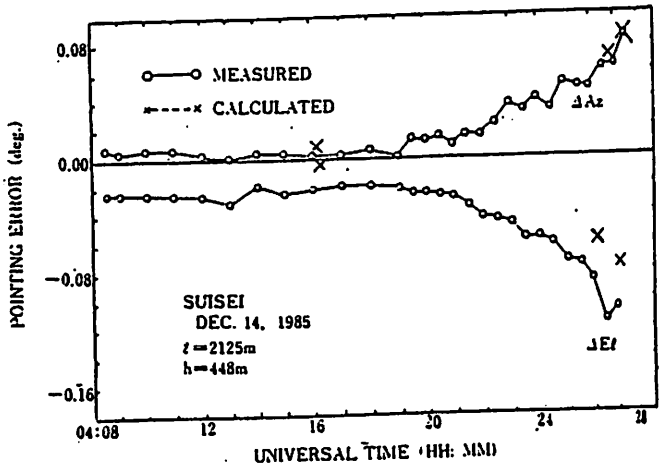

Fig.7 Antenna pointing error at LOS

Theoretical analysis

The situation of reception at the low elevation angle is shown schematically in Fig.8 with parameters used in the following analysis. The radio wave from the spacecraft is blocked by the mountain ridge and forms the shadow on the aperture with the boundary designated A2. The shadow boundary is almost horizontal because the size of terrain is far larger than the aperture. The distance of A2 measurefd upward from the aperture center O changes from a to ∞ a(a:aperture radius) when the shadow vanishing.

The radiation pattern F(Az,El) from the field distribution f(r,θ) on the illuminated portion of the aperture S is expressed by,

$$F(Az,El)=\iint_S f(r,\theta)e^{jkr\sin\theta}rdrd\theta. \quad (1)$$

Let f(r, θ) be the field pattern of TE11 mode in a circular waveguide with phase change due to antenna offset. This assumption is not true in general, but expresses real distribution in some cases[3].

The computed result of Eq.(1) is shown in Fig.9 with the coordinate of shadow a2. In case of clear aperture(a2=-32), the curves represent the radiation patterns of TE11 mode from a circular waveguide. According to shadowing, the level decreases gradually and the beamwidth becomes wider.

Figure 9 shows also the radiation pattern from a rectangular aperture with uniform illumination. The curves agree fairly well with TE11 mode radiation patterns as long as the field strength is more than -4 dB of the peak level and at small offset angle. This range of applicability is acceptable to consider the

antenna operation.

For the distance l and height h of the mountain ridge, a2 is expressed by Eq.(2) after simple calculation.

$$a2=(h-c-l*\tan El)*\cos El \qquad (2)$$

Therefore, reception level can be calculated against El considering phase disribution on the aperture with a parameter of offset angle.

The result is shown in Fig.10 with measured data translated from Fig.5 and Fig.6. They agree well each other, except for the lowest data in Fig.10(b) which is out of applicability of Fig.9 for a2=10. The level changes at the low elevation angle are, therefore, explained by simple geometrical shadowing of the aperture.

The 3 dB decrease condition of each set of l and h is calculated using Eq.(2). The result is shown in Fig.11 which can be used to estimate the margin of antenna operation time at AOS and LOS.

The pointing error shown in Fig.7 can not be explained by the simple geometrical shadowing model, but the behavior of the autotrack system which uses TM01 mode and TE01 mode as tracking modes should be analyzed. Corresponding to the modes in the antenna feeder under consideration, let the aperture field distribution be approximated by the same mode in the circular waveguide of the same radius as the aperture.

The induced mode is calculated from Eq.(3) using the orthogonality of modes.

$$fin(r,\theta)=a1*mTE11+a2*mTM01+a3*mTE01+\sum_{i\geq 4} ai*mi \qquad (3)$$

where fin is the incident field on the aperture with phase correction due to oblique incidence, m is the specific distribution function of the mode indicated by the suffix, and ai is the mode ampltude.

Linearly polarized wave is examined first, and then characteristics in circular polarization are infered.

Generated amount of one of the tracking modes TM01 is shown in Fig.12 for vertical(V-)polarization port and horizontal(H-) polarization port of the mode coupler. At the boresight, there is no output from H-polarization port. On the other hand V-polarization port generates finite output even at the boresight if there is shadow on the aperture.

TE01 mode is induced in the complementary sets of both polarization and plane. In reality the strength of the error signal is given by the field strength of both tracking modes normalized by the

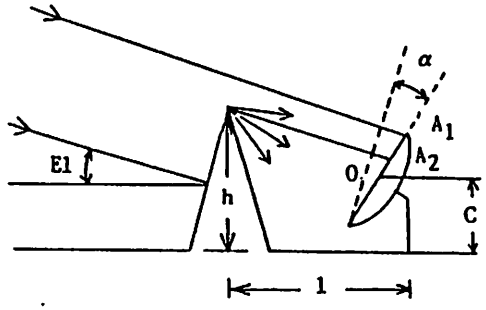

Fig.8 Schematic view of reception situation

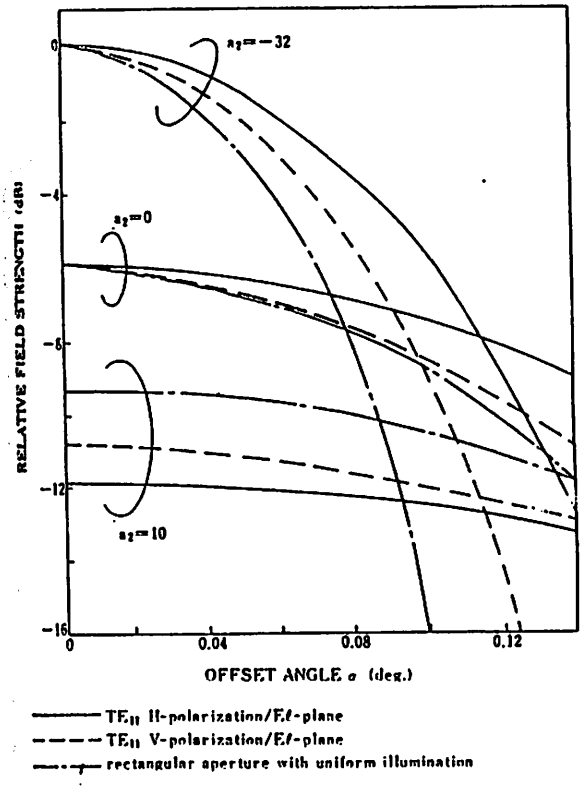

Fig.9 Radiation patterns of model antennas

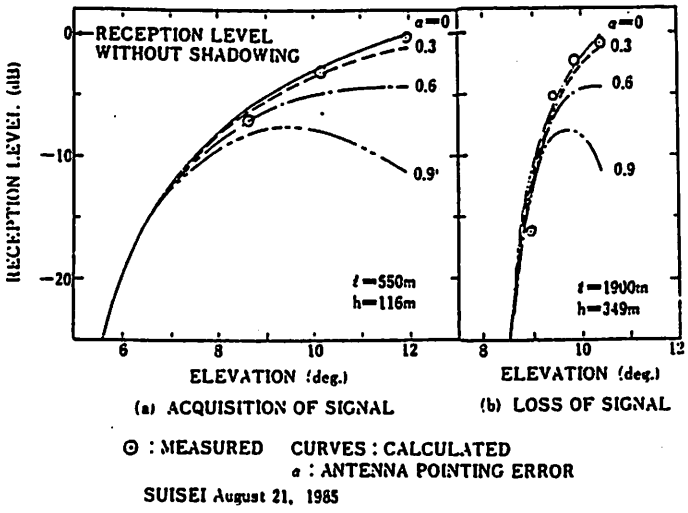

Fig.10 Theoretical power level change at AOS and LOS

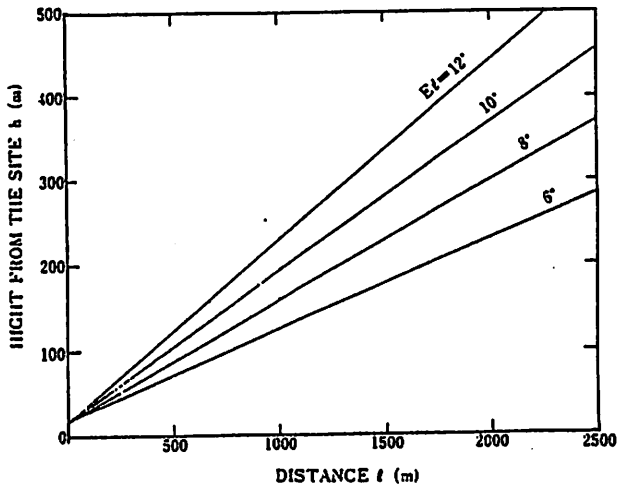

Fig.11 3 dB decrease condition of h and l with a parameter of El angle

level of the reference mode TE11. The antenna is driven to the equilibrium point which corresponds to the intresection of curves in Fig.12 for each polarization and plane.

The direction of the antenna driving force is expressed by the phase of the combined wave of TM01 mode and TE01 mode relative to TE11 mode.Therefore, the phase of tracking modes relative to the reference mode should be analyzed . The result showed that the phase of TM01 mode is retarded to TE11 mode by 90 deg. in the case of little shadow.

When half of the aperture is shadowed(a2=0), the computed results are shown in Fig.13 where IC and IS represent the real and imaginary parts of the mode amplitude. TM01 mode and TE11 mode for H-polarization have sinmilar phase characteristics to the case of little shadow. But both modes for V-polarization draw the phase loci with El angle as shown in Fig.13(b), and the phase of TM01 mode is retarded to that of TE11 mode by 180 to 140 deg. according to the offset angle. The phase of TE01 mode relative to TE11 mode shows similar change to TM01 mode except that the polariztions are reversed. Therefore, antenna driving force for a2=0 directes between 0 to 45 deg. from the Az axis.

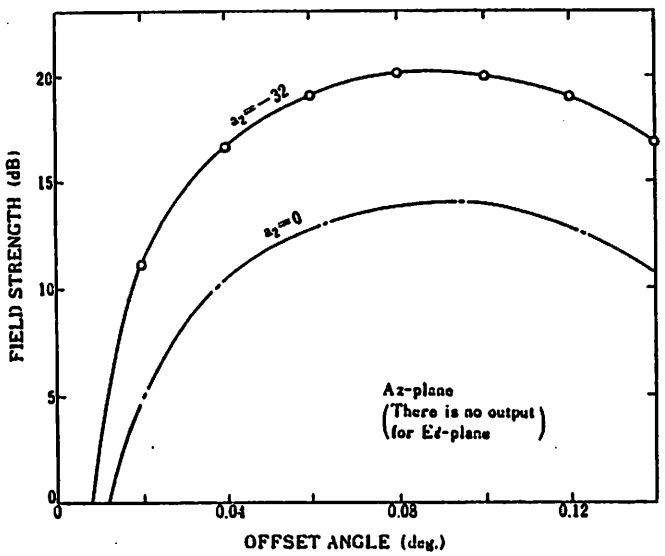

(a) H-polarization

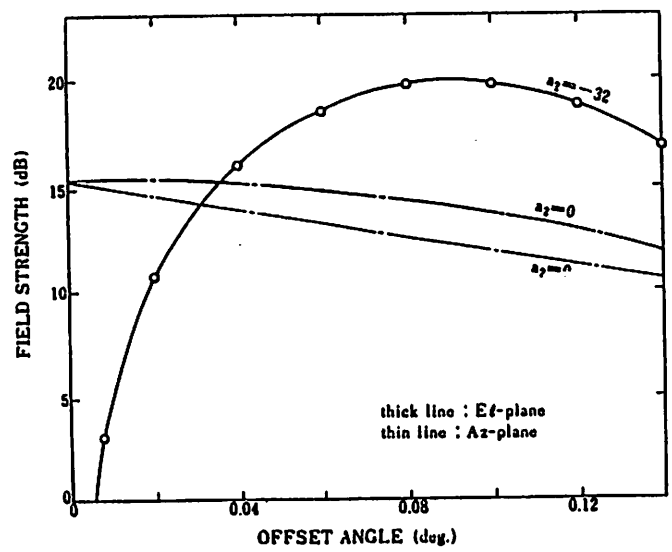

(b) V-polarization

Fig.12 Generation of TM01 mode for two polarizations

The cross coupling between the axes of Az and El is neglected until now, but there is certain amount of coupling. And the incident field is elliptically polarixed in general. Probably for these reasons, the antenna was driven almost equally in El and Az. In this case the calculated values are marked in Fig.7. They show good coincidence with measured data.

Conclusion

The change of reception level at the low elevation angle is explained well by simple geometrical shadowing of the aperture. The results are feasible for the determination of operation schedule of gigantic antennas for each field. The behavior of autotrack system with shadow on the aperture is analyzed. The use of the system may cause pointing error of the antenna at the low elevation angle.

Acknowledgement

The authors thank Mr.M.Yamada for doing experiments.

References

[1]T.Nomura et al. "Usuda deep space station with 64-meter-diameter antenna", in Proceedings of 36th IAF Congress,IAF-85-381,1985.
[2]J.S.Cook and R.Lowell,"The autotrack system", B.S.T.J.,pp.1283-1307,July 1963.
[3]S.Silver, Microwave Antenna Theory and Design. New York: McGraw-Hill, 1949,pp336-341.

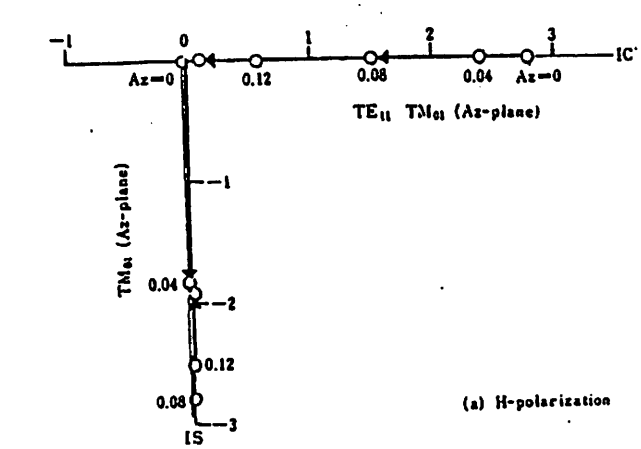

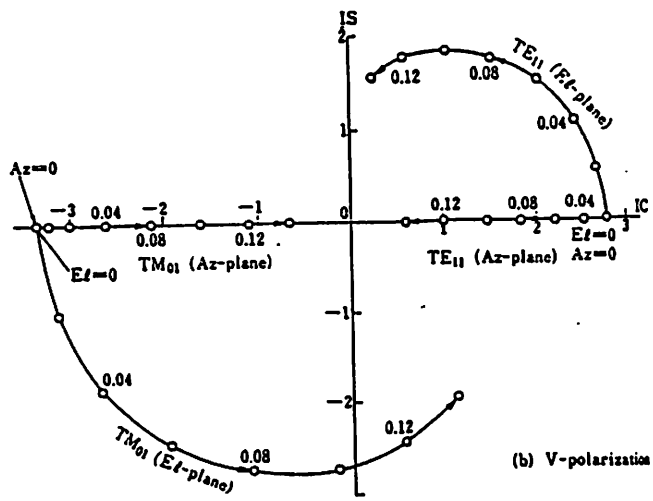

Fig.13 Phase diagram of a tracking mode TM01 relative to the reference mode TE11